Shadia Ikhmayies *Editor*

Advances in Silicon Solar Cells

Springer

Advances in Silicon Solar Cells

Shadia Ikhmayies
Editor

Advances in Silicon Solar Cells

Springer

Editor
Shadia Ikhmayies
Department of Physics
Al Isra University
Amman, Jordan

ISBN 978-3-319-69702-4 ISBN 978-3-319-69703-1 (eBook)
https://doi.org/10.1007/978-3-319-69703-1

Library of Congress Control Number: 2017963208

Printed on acid-free paper

This Springer imprint is published by Springer Nature
The registered company is Springer International Publishing AG
The registered company address is: Gewerbestrasse 11, 6330 Cham, Switzerland

Contents

Organic–Inorganic Hybrid Silicon Solar

Yingfeng Li, Younan Luo, and Meicheng Li

Abstract The real challenge of solar cells can be summarized to reduce the cost while increasing the conversion efficiencies. Organic–inorganic hybrid silicon solar cell is a newly developed type of solar cells which is expected to realize above requirement. It can inherit the high efficiency and reliability of the silicon material and the flexibility, light weight, and affordability of the organic materials. In this new type of devices, an organic layer is generally spread on the silicon to form the heterojunction, where the silicon wafer is adopted as the optical absorber. To reduce cost, ultrathin silicon wafer should be the best choice if only it can absorb enough sunlight to support the high efficiency. Therefore, light-trapping nanostructures, like silicon pyramid, nanowire, nanocone, and silver nanoparticle, have been widely utilized to improve the light absorption. As a consequence, the preparation of ultrathin silicon wafer and various silicon nanostructures is an important fundamental for the organic–inorganic hybrid silicon solar cells. In addition to form heterojunction with silicon, the other function of the polymer layer is to transport holes. So, the hole-transporting ability is one of the main criteria for choosing the polymer. In these days, PEDOT:PSS is most widely used and thought to be the best choice. Because silicon is inorganic, it is a challenge to form a perfect interface contact with the PEDOT:PSS; thus, there always exists abundance of defect structures and defect states on the organic–inorganic interface. These interface defects are another limitation for the efficiency of the organic–inorganic hybrid silicon solar cells. So, fabrication technology is another very important aspect to ensure the high efficiency of such type of hybrid solar cells. It includes modifying the surface wettability of silicon to improve the junction quality and importing

Y. Li · Y. Luo
State Key Laboratory of Alternate Electrical Power System with Renewable Energy Sources, North China Electric Power University, Beijing, China

M. Li (✉)
State Key Laboratory of Alternate Electrical Power System with Renewable Energy Sources, North China Electric Power University, Beijing, China

Chongqing Materials Research Institute, Chongqing, China
e-mail: mcli@ncepu.edu.cn

S. Ikhmayies (ed.), *Advances in Silicon Solar Cells*,
https://doi.org/10.1007/978-3-319-69703-1_8

effective passivation for the organic–inorganic interface to reduce the recombination centers. Considering these factors, in this chapter, firstly, some recent works on the preparation of crystal silicon membrane and several silicon nanostructures have been summarized by us; then, the basic process, especially the passivation technologies, in fabricating the heterojunction is given. We hope this summary is helpful for the future development of organic–inorganic hybrid silicon solar cells.

1 Introduction

The real challenge of solar cells can be summarized to reduce the cost while increasing the conversion efficiencies. Within current types of solar cells, silicon-based devices dominate the market with over 80% share due to high efficiency, reliability, and nontoxic Earth-abundant resources. However, the purification and fabrication processes of solar-grade silicon are costly, which make for approximate 75% of the total cost. Additionally, the purification process of silicon is very energy consumed and therefore caused deleterious environmental consequences. Despite the thin-wafer or thin-film technologies used recently in the photovoltaic industry, actually, they can't solve the problem significantly.

The organic solar cell is another potential kind of photon-electric conversion devices. They have several advantages, including mechanical flexibility, lightweight, and simple production process under low-temperature; can be produced in arbitrary colors; etc. The most crucial problem for this kind of photovoltaic device is the low carrier mobility and conductance of organic materials. These cause abundant carrier recombination thus low device efficiencies even for laboratory cells. Besides, stability is another problem that can't be neglected for the organic solar cells.

Organic–inorganic hybrid silicon solar cell offers a practical means to reduce fabrication cost while getting considerable power conversion efficiencies. The device structure of organic-inorganic hybrid silicon solar cells is rather straightforward. Conjugated polymers are spread on a silicon surface with low-temperature and soluble processes; thus, a heterojunction can be formed. Therefore, the power conversion efficiency of such type of photovoltaic devices is fundamentally determined by three main factors: (1) the optical absorption in the silicon absorber [1], (2) the hole transport in the organic layer [1], and (3) the carrier recombination on the silicon–organic interface [2].

Crystalline silicon thin membranes are generally adopted as the optical absorber in organic–inorganic hybrid silicon solar cells, in order to reduce cost; and for photon trapping, silicon nanostructures including silicon pyramids, silicon nanowires, and silicon nanocones have to be fabricated on the thin membrane [3, 4]. It has been demonstrated that the hole mobility in PEDOT:PSS is much higher than that of most other polymers [4]; so, PEDOT:PSS is the mostly used organic material in the organic–inorganic hybrid silicon solar cells, and actually, the thickness of the PEDOT:PSS layer is generally limited to about 100 nm to

reduce the transport distance of hole in it as far as possible. The carrier recombination on the silicon–organic interface is a key scientific problem [2]; therefore, the passivation for this interface attracts increasing attentions [2, 5, 6]. Some passivation technologies, like natural oxidation, methylation, and amorphous silicon layer, have been proposed.

In this chapter, the preparation of crystalline silicon membrane and several silicon nanostructures, which are of great importance for the fabrication of flexible, low-cost, and high-efficiency organic–inorganic hybrid silicon solar cells, will be first introduced. Then, the basic fabrication process of organic–inorganic hybrid silicon solar cells will be given, especially the passivation technologies for the silicon–organic interface. For organic–inorganic hybrid silicon solar cell, the passivation technologies are the bottleneck to boost the efficiency.

2 Fabrication of Silicon Membrane and Silicon Nanostructures

2.1 Ultrathin Silicon Wafer

The ultrathin silicon wafer is the basis for the fabrication of low-cost organic–inorganic hybrid silicon solar cell. Till now on, the available fabrication technologies for ultrathin silicon wafer can be generally divided into two classes: mechanical cutting + grinding method and chemical etching method. However, using the former technology, it is difficult to obtain silicon wafers with a thickness less than 100 μm; and it will import damage layer 0.2–2.0 μm, as shown in Fig. 1 [7].

The chemical etching method is the most advanced method to fabricate ultrathin silicon wafer till now. It is a simple, low-cost, and low-damage method. Using this method, the silicon wafer can be reduced to be several micrometers, and the thickness can be easily controlled by just adjusting the etching conditions and/or

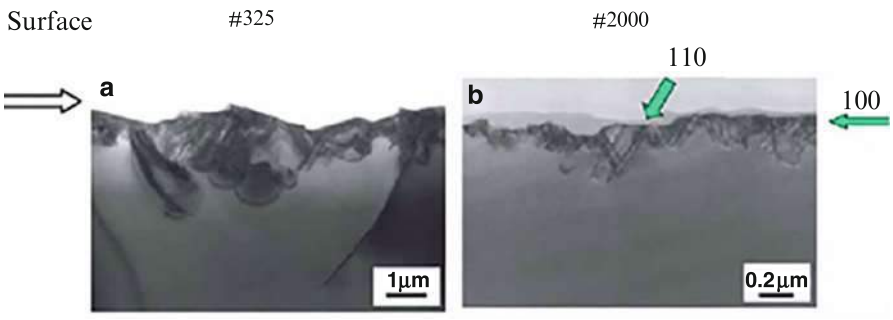

Fig. 1 TEM image of monocrystalline silicon surface defects ground by traditional grinding method [7]. (**a**) Ground by 325 mesh powder; (**b**) ground by 2000 mesh powder

etching time. According to the composition of the etchant, the chemical etching method can be classified into acid etching and alkaline etching methods.

For acid etching, the etching solution contains HF, $AgNO_3$, H_2O_2, and H_2O. The actual etching is a metal-assisted chemical etching (MACE) process [8]. When the silicon wafer is immersed into the etching solution, the Ag^+ ions can seize electrons from the valence band of silicon and thus form Ag nucleation which gradually grows into Ag nanoparticles. After that, the formed Ag particles will act as the catalyst: the Ag particles will seize electrons from the regions of silicon wafer contacting with or around them; the seized electrons will reduce the H^+ at the surface of Ag, and the holes will be consumed by the oxidation of silicon. The reaction equations can be summarized as follows [8]:

Reaction at metal (cathode)

$$H_2O_2 + 2H^+ \rightarrow 2H_2O + 2h^+ \text{and } 2H^+ + 2e^- \rightarrow H_2 \uparrow \quad (1)$$

Reaction of Si etching (anode)

$$Si + 4h^+ + 4HF \rightarrow SiF_4 + 4H^+ \text{and } SiF_4 + 2HF \rightarrow H_2SiF_6 \quad (2)$$

From these equations, it can be seen that H_2O_2 can increase hole injection rate thus leading to high etching rate. Another important feature in the MACE of silicon is that the reaction rate shows great crystal orientation selectivity [9, 10]. This is because the bond density along the different directions of silicon is quite different. It has been demonstrated that the anisotropy in MACE of silicon can be effectively regulated by the etchant concentration [11, 12].

Through adjusting the ratio of the HF, $AgNO_3$, and H_2O_2, Bai et al. [13] have realized the fabrication of ultrathin silicon wafer using the MACE method. They have obtained ultrathin silicon wafer with a thickness about 30 μm, as shown in Fig. 2. However, since the intrinsic anisotropic etching feature, the surface quality of the obtained ultrathin silicon wafer is not very well. The average roughness is about 13 nm. Besides, some Ag nanoparticles will be left on the surface of the ultrathin silicon wafer after etching, which will affect the performance of solar cells fabricated.

Alkaline etching is a more simple method compared with the acid etching method [14–17]. In this method, the standard silicon wafer simply needs to be immersed in an alkaline solution for sometimes to fabricate the ultrathin silicon wafers. The reaction mechanism in alkaline etching process can be briefly summarized as [18]

$$KOH + H_2O \longrightarrow K^+ + 2OH^- + H^+ \quad (3)$$

$$Si + 2OH^- + 4H_2O \longrightarrow Si(OH)_6{}^{2-} + 2H_2 \uparrow \quad (4)$$

When we put the silicon wafer into the solution, the silicon atoms on the surface of the wafer will react with the OH^- forming the complex $Si(OH)_6{}^{2-}$. Such complex is easy to be dissolved into water. What are given in Fig. 3 are the ultrathin

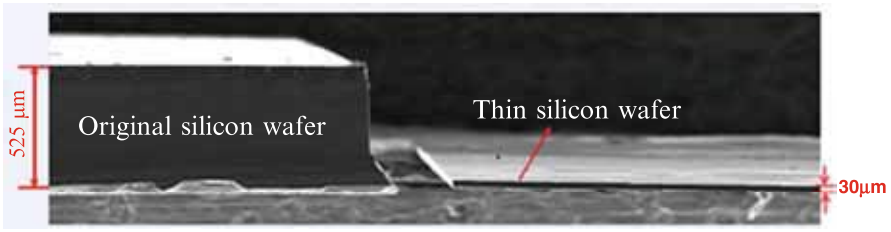

Fig. 2 Cross-sectional SEM image of the contrast on the thicknesses of the original silicon wafer and the acid thinned ultrathin silicon wafer

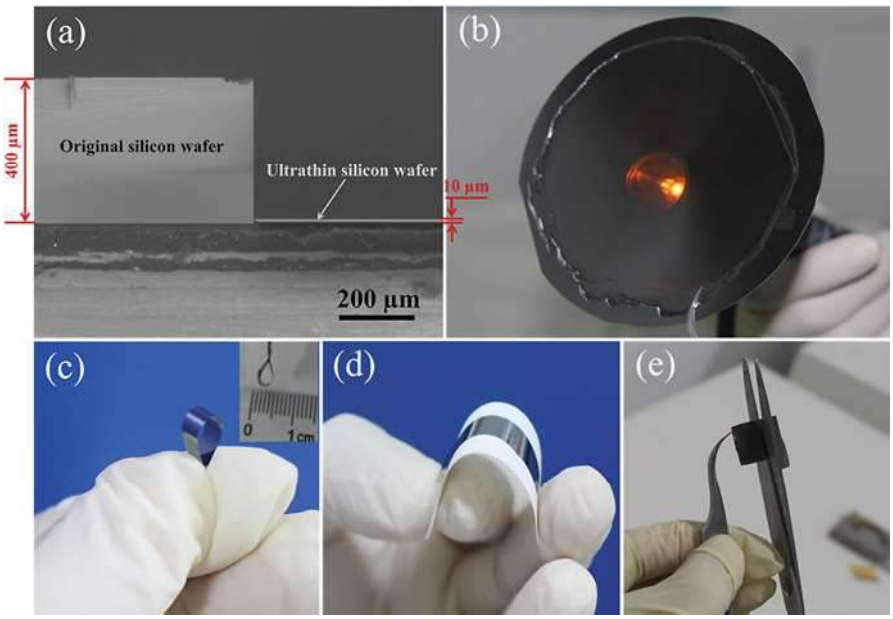

Fig. 3 Contrast on the thicknesses of the silicon wafers before and after the alkaline solution thinning process and the physical properties of the ultrathin silicon wafer. (**a**) Cross-sectional SEM image of the silicon wafers before and after thinning; (**b**) 4-inch ultrathin silicon wafer; (**c**) flexibility of the ultrathin silicon wafer without substrate; (**d**) flexibility of the ultrathin silicon wafer with the substrate; (**e**) ultrathin silicon wafer's cutting

silicon wafers fabricated using the alkaline etching method with a thickness about 10 μm. It can be seen that the silicon wafer of this thickness can transmit orange light, and it shows very good mechanical flexibility. Its radius of curvature reaches about 2 mm. This indicates the organic–inorganic hybrid silicon solar cells based on such ultrathin silicon wafer can also have good mechanical flexibility.

Besides, using alkaline etching method, the ultrathin silicon wafer can be reduced to about 2 μm, and the thickness can simply be controlled by adjusting the concentration of the solution, the reaction temperature, and the time. Figure 4

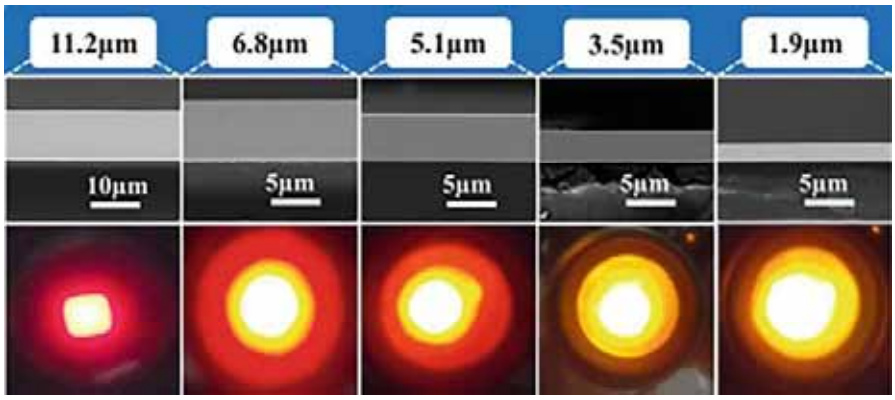

Fig. 4 Corresponding relationship between the colors of the lights getting through the ultrathin silicon wafers and their thicknesses

shows silicon wafers with several thicknesses from 1.9 μm to 11.2 μm and their corresponding light transmission properties. The light transmission properties reflect the light absorption ability of the silicon wafers. This means that how much solar light can be effectively absorbed in the organic–inorganic hybrid silicon solar cells based on the ultrathin silicon wafer can be estimated according to these figures.

Additionally, the surface quality of ultrathin silicon wafer fabricated by alkaline etching method is much better than that fabricated by the acid method. As shown in Fig. 5, the average roughness of the sample obtained by the alkaline etching method is about 0.15 nm, which is quite smaller than that by the acid etching method, 13.8 nm.

The better surface quality of the ultrathin silicon wafer fabricated by alkaline etching method can be mainly attributed to two reasons. The first one is that, although the alkaline etching is anisotropic determined by the fact that the number of Si–Si bonds along different crystalline directions are different, the reaction is a homogeneous process. This is because there are no metal particles acting as the reaction centers during the etching process due to that the alkaline solution is only composed of potassium hydroxide and DI water. The second one is that the etching rate of alkaline etching is much lower than that of acid etching. For the acid etching, at a low temperature about 40 °C, the etching rate can also reach about 48 μm/min. However, for the alkaline etching, even at a high temperature about 90 °C, the etching rate is only about 1.3 μm/min.

It has demonstrated that adding isopropyl alcohol or n-butyl alcohol into the alkaline etching solution as protectant is also helpful for obtaining samples of high surface quality [14–17]. However, we have not found the similar results. The samples fabricated with no protectant, with isopropyl alcohol added and n-butyl alcohol added, are given in Fig. 6. The results show that the ultrathin silicon wafer with no protectant owns the best surface quality.

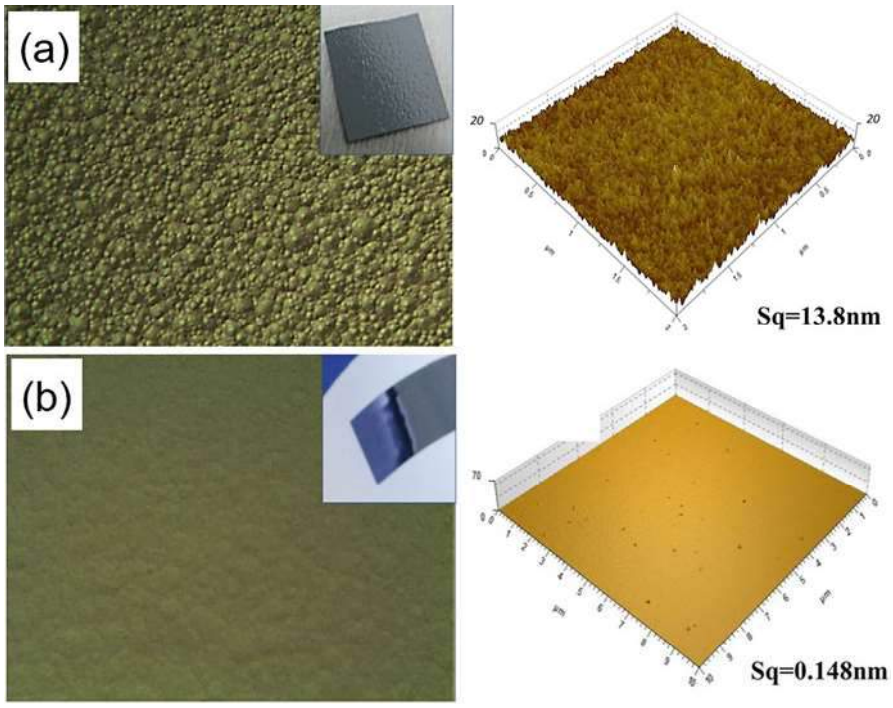

Fig. 5 Optical micrograph and AFM image of ultrathin silicon wafer fabricated by the (**a**) acid etching and (**b**) alkaline etching method, respectively. The amplification factor of the optical micrographs is 200 times. Sq means the surface root mean square roughness

2.2 Silicon Nanostructures

Fabrication of silicon nanostructures is another basic process for organic–inorganic hybrid silicon solar cells, which undertake the responsibility to improve light absorption. Silicon pyramid, silicon nanowire, and silicon nanocone are the three most popular silicon nanostructures for light absorption enhancement. Therefore, the recent progress on the fabrication of them will be summarized next.

2.2.1 Silicon Pyramid

Silicon pyramid is the anti-reflectance structure used currently in industrial crystal silicon solar cells. After the silicon pyramid being fabricated, the reflectance of the crystal silicon surface can be reduced to about 11% from 40% (polished silicon) [19]. Such an anti-reflectance effect is not very good, but there are many advantages for the silicon pyramid structure.

The main merit of silicon pyramid is that the fabrication process is very simple and cheap. It can be fabricated by immersing the crystalline wafer into alkaline

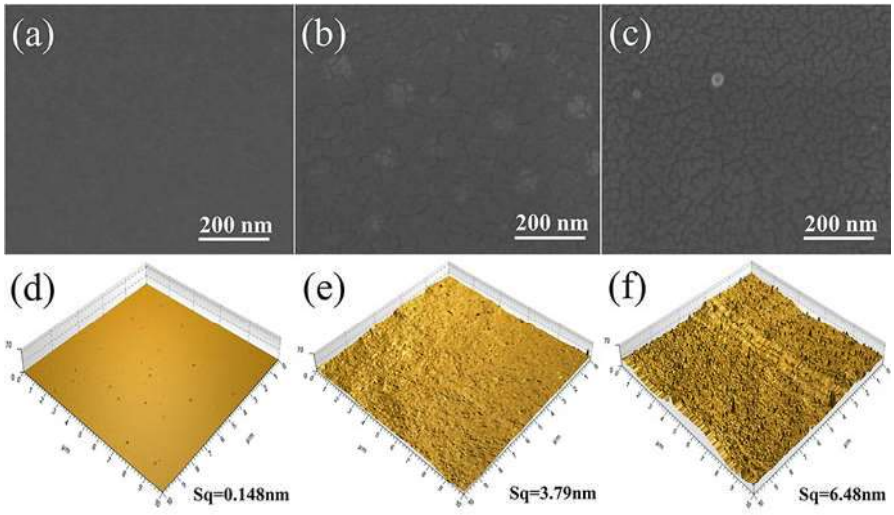

Fig. 6 SEM (upper) and AFM images for ultrathin silicon wafers thinned without a protective agent and with different protective agents in alkaline solution. (**a**) and (**d**) without a protective agent; (**b**) and (**e**) with isopropyl alcohol; (**c**) and (**f**) with butyl alcohol

solutions with solutes NaOH, KOH, $NaHCO_3$, $NaCO_3$, and $NaSiO_3$. The details can be found everywhere. The formation of a pyramid structure occurs because the bond density on (100) crystal surface is much lower than that on (111) crystalline surface. Therefore, during the etching process, the silicon atoms on (100) surface easily tend to be removed but the ones on (111) surface tend to remain. Figure 7a shows the SEM image of silicon pyramid structure fabricated using the KOH solution. We also found that hierarchical silicon pyramid structure can be fabricated through controlling the concentration of KOH and the etching time, as given in Fig. 7b [20].

Another advantage of silicon pyramid utilized in organic–inorganic hybrid silicon solar cells is its better surface quality compared as other silicon nanostructures will be introduced below. This is attributed to the low height (the general height of the silicon pyramids is about 5 μm) and large tilt angle (the tilt angle is fixed to 30.3°). These features ensure that all the small facets of the pyramid are exposed and there is no sharp valley on the silicon surface. High surface quality is very helpful to obtain high conversion efficiency in photovoltaic devices.

Besides, the low height and large tilt angle can also contribute to fabricate high-quality organic–inorganic contact interface directly on the silicon pyramid surface. That is, an organic layer can be directly spun-coated on the silicon pyramid surface to fabricate the heterojunction. This is of great significance since the good filling of organic materials into silicon nanostructures is one of the biggest challenges for fabricating organic–inorganic hybrid silicon solar cells with high efficiency. In this point of view, the hierarchical silicon pyramid we fabricated should be of the promising application as the hierarchical structure can catch the organic materials more tightly.

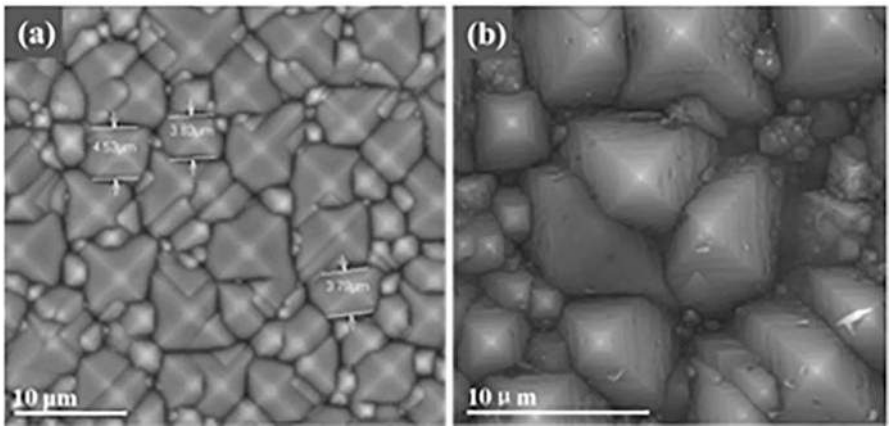

Fig. 7 SEM images of (**a**) silicon pyramid and (**b**) hierarchical silicon pyramid structures etched in KOH solution

2.2.2 Silicon Nanowire

Silicon nanowire exhibits much better light-trapping efficiency than silicon pyramid structures. It can reduce the reflectance of the silicon surface to 2% even lower [20–23]. Such an excellent anti-reflectance function of silicon nanowire is obviously very important for solar cells, thus attracting great attentions.

For the fabrication of silicon nanowire, generally, there are two types of methods, the bottom-up and top-down ones. The "vapor–liquid–solid" (VLS) growth is a representative method of the bottom-up scheme [24–29]. Using this method, relatively high-quality silicon nanowires with controllable length and diameter can be fabricated. The top-down scheme can then be divided into dry and wet etching approaches. The inductively coupled plasma (ICP) etching is the most commonly used dry etching approach [30, 31], and using any of them, the density and size of silicon nanowires can be strictly controlled. However, no matter the VLS or the ICP methods require large facility and high energy consumption. Therefore, they are both not suitable for large-scale applications in preparing materials for the organic–inorganic hybrid silicon solar cells. The MACE method is a typical wet etching approach with special advantages for industrial applications [32–40]. It only requires very simple equipment, the reaction temperature is lower than 100 °C, and meanwhile the shape, size, and surface quality of the samples are controlled. As a consequence, the MACE technique is thriving day-by-day advancing to a level where silicon nanowire of the desired shape, size, and surface quality can be readily fabricated.

When using silicon nanowire for light trapping in solar cells, there are several factors that need to be considered. The surface density is the first important factor as silicon nanowire has excellent light concentration ability. According to our numerical simulations [41], a single silicon nanowire can collect light in the area more

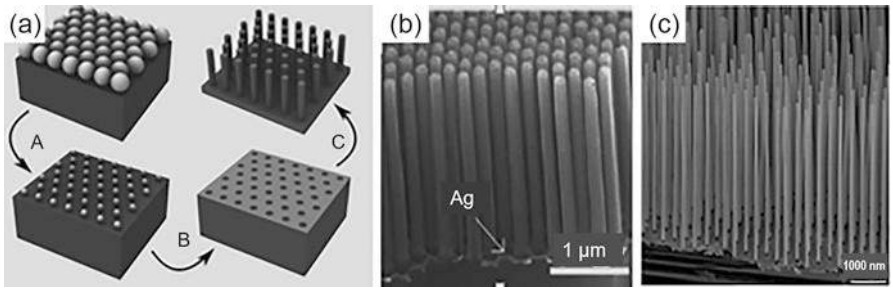

Fig. 8 (**a**) An illustration of the template method in MACE using PS spheres as the mask [42] and silicon nanowire arrays of (**b**) high [43] and (**c**) low surface densities [44]

than 300 times of its geometrical cross-sectional area due to leaky mode excitation. This means the silicon nanowire array with fill fraction $<5\%$ can achieve near-unity broadband absorption. Therefore, it is unnecessary to fabricate compact silicon nanowire array to trap light for the organic–inorganic hybrid silicon solar cells, which will conversely hinder the filling of PEDOT:PSS in it, and bring in a large number of defects.

The surface density of silicon nanowires can be effectively controlled by the so-called template method in MACE, where PS sphere is the most popular used as the mask [42]. An overall process is illustrated in Fig. 8a, where (I) the PS spheres are firstly assembled on the silicon surface, (II) then an RIE process is carried out to form the spacing, (III) after that an Ag thin film is deposited and the PS spheres are removed, and (IV) finally the silicon nanowire array is obtained by MACE. In such template method, the surface density of the silicon nanowires can be controlled by the diameter of the PS spheres and the RIE time. Silicon nanowire arrays of high and low surface densities obtained by this method are shown in Fig. 8b, c [43, 44].

Diameter is another important parameter for the light-trapping effect of silicon nanowire array. Our simulation results demonstrated that silicon nanowire with diameter ~80 nm owns the best light-trapping ability [45]. As reflected in Fig. 9, the resonant wavelength (peak position) for silicon nanowire of diameter 80 nm corresponds to the maximum irradiance in the AM1.5G spectrum; and silicon nanowire with 80 nm diameter puts up the best light-concentration ability at the resonant wavelength (peak intensity).

Diameter can be also perfectly controlled by the above template method by adjusting the RIE time. However, it is unnecessary to use a so complex method to control the diameter of silicon nanowire. In MACE of silicon using no template, the diameter of the obtained nanowire can be generally controlled by adjusting the deposition process in fabricating the catalyst (silver film, usually fabricated by the magnetron sputtering). In our experiments and Leonard et al. report [46], the diameter of the silicon nanowires can be controlled to a range 50–100 nm [47]. Recently, through the more specific process, Um et al. [48] have controlled the diameter of the silicon nanowires to a range 60–90 nm.

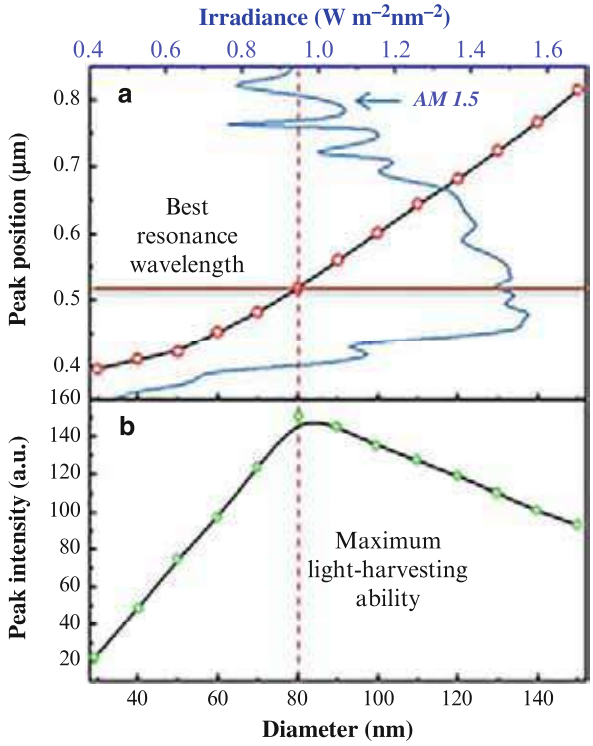

Fig. 9 The (**a**) resonance wavelengths and (**b**) corresponding light-concentration abilities of silicon nanowires with different diameters

Length is also a very important parameter since it dramatically determines the amount of light being absorbed in the silicon nanowires themselves. For photovoltaic devices with a p–n junction in the bulk part of the silicon substrate, a balance between the light-trapping ability of the silicon nanowires and the amount of light being absorbed themselves must be considered. For solar cells with the radial junction, there will be a specific length of the silicon nanowire to achieve the optimized light absorption efficiency. The simulation results indicate that the silicon nanowire with length 3 μm owns the optimal light absorption efficiency [49]. By comparing the photovoltaic output characteristics of radial p–n junction solar cells fabricated on silicon nanowires with different lengths, Yang et al. demonstrated that the enhanced light absorption in silicon nanowires with length ranging from 2 to 5 μm can dominate over surface carrier recombination [50]. In our MACE, we found that the length of silicon nanowire is nearly linear with the reaction time even under different temperatures, as shown in Fig. 10. Therefore, the length of silicon nanowire can be simply controlled by the etching time.

Due to the excellent light-trapping ability, a silicon nanowire is of great promise to be used for conquering the inadequate light absorption in organic–inorganic hybrid silicon solar cells. Besides, the numerical simulation results have demonstrated that the collected light by silicon nanowire shows up very significant skin effect [21]. That is to say, most of the collected light will be localized near the

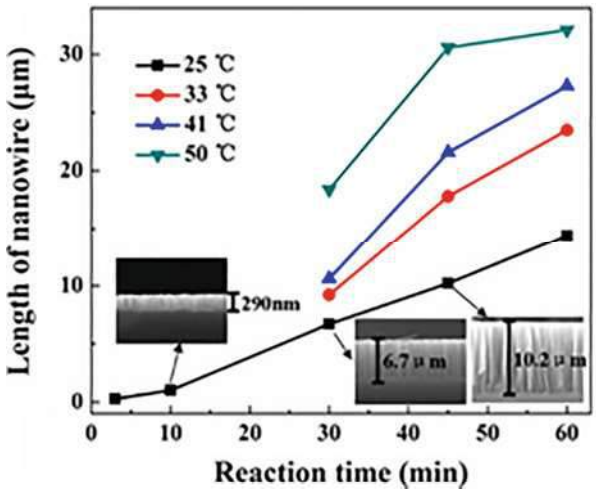

Fig. 10 Relation of silicon nanowire length and reaction time at different temperatures

surface of the nanowire, which means silicon nanowire structure is very suitable to be used in radial junction photovoltaic devices. The PCE of organic–inorganic hybrid silicon solar cells with such radial junction architecture has reached to 13.6% [51]. However, since the inevitable metal residual and defects in silicon nanowire fabricated by MACE and the difficulty in filling organics in the nanowire structure, the fabrication of radial organic–inorganic hybrid silicon solar cells with higher efficiency is still a great challenge.

2.2.3 Silicon Nanocone

Silicon nanocone is another nanostructure of excellent light-trapping ability, which can be fabricated with the similar process as silicon nanowire. Besides, its shape is similar as silicon nanowire with great aspect ratio; thus, it is also called as tapered silicon nanowire elsewhere. The light-trapping effect of silicon nanocone is even better than nanowire [52, 53]; therefore, its fabrication and application attract great attentions.

Lin et al. [54] have developed a process to fabricate silicon nanocone with uniform shape and regular arrangement, as shown in Fig. 11a, b. However, this process is quite complex which needs a Ti/Au mesh film as the mask and several repeated processes of depositing catalysts and etching. As an improvement, Bai et al. [55] have developed a one-step template-free method to fabricate silicon nanocone. The only thing to do is to immerse the silicon wafer with deposited silver film in the HF/H_2O_2 solution. In their report, silicon nanocone array with length ~400 nm and continuously various diameters from 5–10 nm to 80–107 nm (tapering degree about 12.7) are obtained, as shown in Fig. 11c, d. The main mechanism of the tapering etching is the in situ oxidative dissolution of the silver network, which means the silver network sinks and dissolves gradually during the etching process.

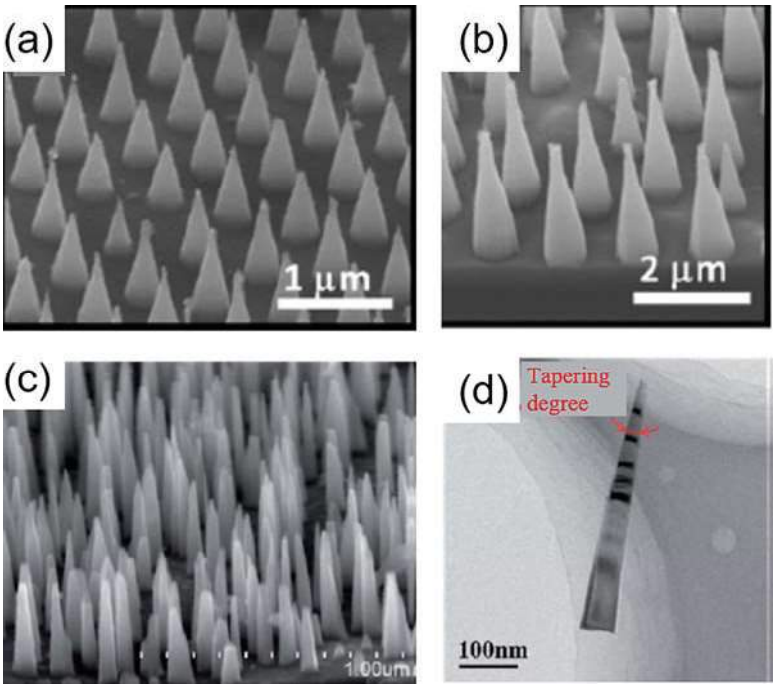

Fig. 11 SEM images of the silicon nanocone fabricated by (**a** and **b** are reproduced from Ref. [54] with permission from The Royal Society of Chemistry) Lin et al. and (**c**) Bai et al. (**d**) TEM image of one individual silicon nanocone in (**c**) (Image **c** and **d** are reproduced from Ref. [55] with permission from The Royal Society of Chemistry)

Besides, Jung et al. [74–76] have demonstrated that silicon nanocone can be also fabricated by etching the silicon nanowire in KOH solution for about 60 s. This should be also a promising method as the processes for fabricating silicon nanowire are mature now.

According to our simulations, due to the continuous diameter variation and resonant wavelengths excited in nanocone, silicon nanocone shows better light-trapping ability than silicon nanowire [53]. Meanwhile, we have found that the average reflectance of a silicon nanocone array with length 1.47 μm in the waveband 300–1000 nm can reach about 1.7%. Taking into account that the tapered feature of silicon nanocone is beneficial for the filling of organics in the interval, silicon nanocone should be also of great application prospect in organic–inorganic hybrid silicon solar cells.

3 Device Fabrication and Passivation

As mentioned in the introduction, fabrication technology is very important to ensure the efficiency of such type of organic–inorganic hybrid solar cells. Following, the basic fabrication process of such hybrid device and point out, the key factors improving the quality of the organic–inorganic hetero junction will be given; and the passivation technologies of the organic–inorganic interface from the recent reports in the device also will be summarized, which is necessary to reduce the carrier recombination.

3.1 Fabrication Process of the Organic–Inorganic Hybrid Silicon Solar Cells

The whole fabrication process can be generally divided into four main steps: cleaning the substrate, modifying the wettability of the silicon surface and PEDOT:PSS solution to improve the quality of heterojunction, fabricating the organic–inorganic heterojunction, and preparing the front and back electrodes.

3.1.1 Substrate Cleaning

Substrate cleaning is the first and very important process in fabricating the organic–inorganic hybrid silicon solar cells. In this step, the physical and chemical adsorbed impurities on the wafer will be removed. The impurities can not only affect the film quality of the organic layer but also bring in abundant carrier recombination. This will dramatically reduce the conversion efficiency and even affect the lifetime or stability of the fabricated organic–inorganic hybrid silicon solar cells. Therefore, a rigid cleaning scheme for the silicon substrate is quite necessary. What's given in Fig. 12 is a mature cleaning procedure technology we used to ensure the formation of the good organic–inorganic interface.

The silicon wafers (N (100), resistivity of 2–4 Ω.cm) are firstly cleaned by acetone (5 min), anhydrous ethanol (5 min), and DI water (10 min) under ultrasonic conditions step-by-step at room temperature. This step aims to remove the organic impurities.

After that, a standard RCA cleaning process is executed [56]. It contains four steps: (a) APM solution (H_2SO_4:30% H_2O_2 = 1:3) is used to clean the surface for 10–15 min, which can remove the organic particles; (b) SPM solution with (NH_4OH:H_2O_2:H_2O) ranging from (1:1:5) to (1:2:7) is used to clean the surface for 10–15 min, which can reduce metal atom pollution; (c) soak the silicon wafer with DHF(HF:H_2O) = 1:(2~10) solution for 5 min to remove the Al, Fe, Zn, Ni, etc. metal particles; and (d) HPM solution with (HCl:H_2O_2:H_2O) ranging from (1:1:6) to (1:2:8) is used to clean the surface for 10–15 min, to remove the Al^{3+}, Fe^{3+}, Mg^{2+}, Zn^{2+}, etc. Besides, in the middle of each cleaning step, the silicon wafer must be

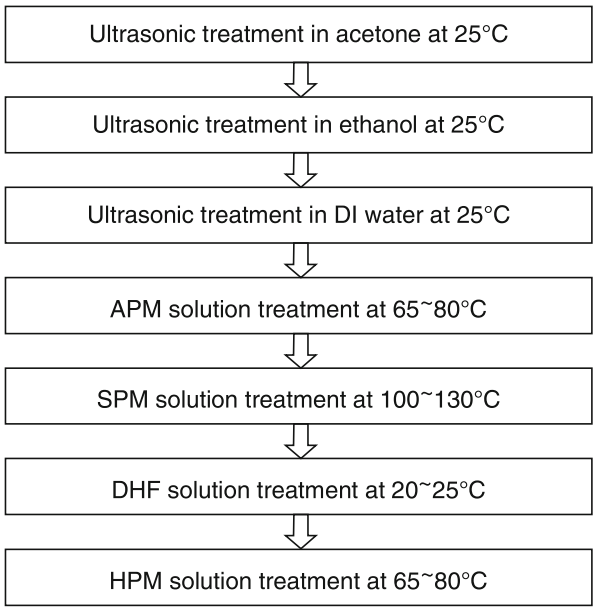

Fig. 12 The cleaning procedure for the silicon wafer

rinsed clearly with super pure water (DI water). This rigid cleaning process can ensure the cleanliness of the silicon wafer reaching a very high degree, which lays a solid foundation for the next experiments. It should be noted that, if such cleaned silicon wafers have been stored for a long time, they are better to be treated by hydrofluoric acid again to remove the oxide layer.

3.1.2 Improve Quality of the Heterojunction

After being cleaned, the surface of the silicon wafer is hydrophobic. So, to form a good heterojunction contact with the hydrophilic PEDOT:PSS, it is required to modify the wettability of the silicon surface. Besides, as the PEDOT:PSS should be dissolved in DI water and then be spin-coated on the surface of the silicon wafer to form heterojunction with silicon, it is also possible to improve the quality of heterojunction by modifying the surface tension of the water solution of PEDOT:PSS.

The hydrophobicity of cleaned silicon surface can be directly reflected by the fact that water dip on the silicon surface exhibits almost spherical: the measured contact angle reaches about 70° [57]. This indicates that it is hard to form flat and homogeneous PEDOT:PSS film through spin coating PEDOT:PSS aqueous solution on untreated silicon. After being oxidized under natural circumstances for 12–24 h, the surface of the silicon wafer changes to be well hydrophilic: a water dip can be spread almost evenly on the silicon surface. This implies the PEDOT:PSS

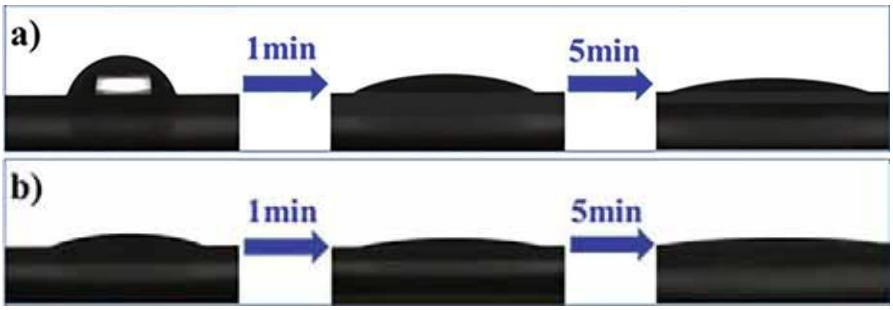

Fig. 13 Influence of Zonyl FSH on the surface tension of PEDOT:PSS solution. (**a**) Before Zonyl FSH addition; (**b**) after Zonyl FSH addition

aqueous solution can be also spun-coated homogeneously on the silicon wafer, to form good heterojunction contact. Besides natural oxidation, the silicon wafer can be modified by the ultraviolet/ozone treatment technology. The ozone atmosphere can increase the oxidized rate dramatically and thus can obtain more uniform oxide layer. Such uniform oxide layer can not only improve the hydrophily of the silicon wafer but also is more effective in reducing the density of surface defects.

Modification on the surface tension of PEDOT:PSS aqueous solution is the other effective method to improve the quality of the heterojunction. According to the reports of Liu et al. [58], added Zonyl FSH (a kind of fluorocarbon surface-active agents) to the PEDOT:PSS solution with 0.1% mass fraction can effectively reduce the surface tension of the PEDOT:PSS solution. As shown in Fig. 13, the spreadability of the PEDOT:PSS aqueous solution can be obviously enhanced after the Zonyl FSH is added. As a result, the surface wetting, leveling, and adhesion of the PEDOT:PSS on the silicon surface are improved. This indicates that the quality of formed heterojunction will be improved after adding appropriate surface-active agents to the PEDOT:PSS water solution.

3.1.3 Fabrication of the Organic–Inorganic Heterojunction

The organic–inorganic heterojunction is generally fabricated by spin coating the PEDOT:PSS aqueous solution on the silicon surface. In this fabrication process, it is very important to control the thickness of the PEDOT:PSS layer. Since the only function of the PEDOT:PSS film is to form a heterojunction with the silicon substrate, the PEDOT:PSS layer should be deposited as thin as possible to reduce the carrier transport distance and to reduce the light absorption loss, so long as no leakage current. Depending on recent researches, the optimal thickness of the PEDOT:PSS layer is about 100 nm.

The thickness of the PEDOT:PSS layer fabricated by the spin-coat process can be controlled by the concentration of the solution and the spin rate, according to the following equation [59]:

$$h_f = KC_0^2/\sqrt{\omega}, \quad (5)$$

where h_f refers to the thickness of the obtained PEDOT:PSS layer, C_0 is the mass concentration of the solution, and ω is the spin rate. For the PEDOT:PSS aqueous solution with concentration of 1.4% (bought from Heraeus, PH1000), a PEDOT:PSS layer of thickness about 100 nm can be obtained under spin rate 3000 rev/min for 1 min according to our experience. A tip is that fabricating PEDOT:PSS layer in the N_2 atmosphere can enhance the performance of the organic–inorganic hybrid silicon solar cells (by about 71.3%) [60]. A reasonable explanation for this enhancement is that the N_2 atmosphere can protect the PEDOT:PSS layer from being polluted.

After the PEDOT:PSS being spin-coated on the silicon wafer, a subsequent annealing process is needed to remove the residual water vapor in the film. Notably, the water vapor has great influence on the performance of the devices. So, in this annealing process, we must ensure the water vapor in the PEDOT:PSS film is completely removed, but avoid the architecture of the organic layer being damaged. Therefore, a balance between eliminating the water vapor and maintaining the structure of PEDOT:PSS must be struck. The usually adopted process is annealing the samples under an N_2 atmosphere at 140–150 °C for about 15 min [61].

Under the same consideration, the annealed organic–inorganic heterojunction (and the final device) should be stored in conditions isolated from water vapor, as PEDOT:PSS has good hydrophilicity. From Fig. 14 it can be seen that the conversion efficiency of the organic–inorganic hybrid silicon solar cells reduces significantly with time when the devices are placed in the natural environment (wet circumstance). After 3 h, the efficiency of device preserved in wet circumstance decreases about 70.8% (from 4.32% to 1.26%). In contrary, the efficiency of device preserved in dry circumstance only decreases about 35.8% (from 4.32% to 2.77%). This comparison proves the great affection of storage environment on the performance of the solar cells.

Doping some functional materials in the PEDOT:PSS should be another effective way to improve the performance of the organic–inorganic hybrid silicon solar

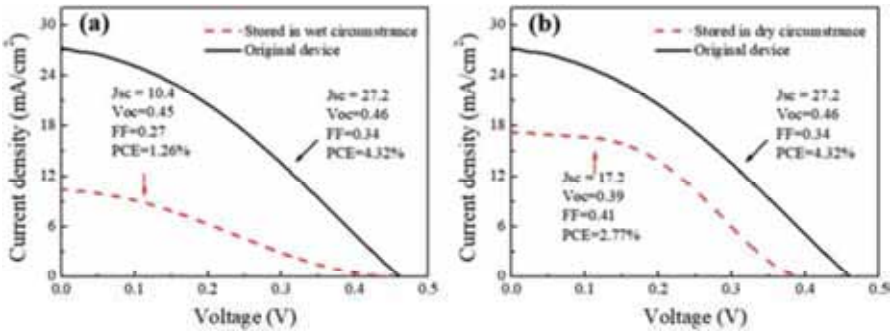

Fig. 14 Comparison between the organic–inorganic hybrid silicon solar cells preserved in (**a**) wet and (**b**) dry circumstance for 3 h

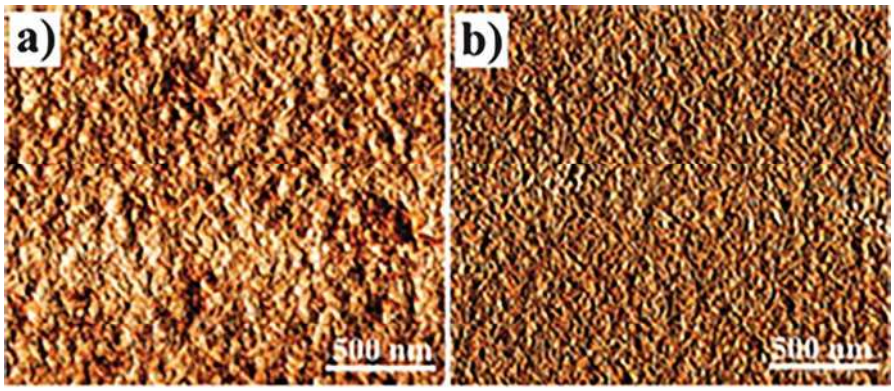

Fig. 15 AFM images of the PEDOT:PSS film. (**a**) Without and (**b**) with DMSO doped

cell. For instance, dimethyl sulfoxide (DMSO) is widely used to dope in the PEDOT:PSS solution. It can make the PEDOT:PSS solution particles more clustered, thus improving the compactness of the organic film. This can be reflected by the average roughness of the film surface as shown in Fig. 15, where the surface quality of the PEDOT:PSS film doped with DMSO has been greatly improved. A compact PEDOT:PSS film is a benefit to forming tight contact with the silicon surface, thus improving the quality of the heterojunction.

The ability to conduct hole is a key property of PEDOT:PSS, which limits the efficiency of the organic–inorganic hybrid solar cells. It has been found that to dope some functional materials can dramatically improve the conductivity of PEDOT:PSS. As reported by Chou et al. [62], the conductivity of PEDOT:PSS can be increased by two orders of magnitude by doping the volume fraction of 5% of DMSO in the PEDOT:PSS solution. Meng et al. [63] have found that adding ZnP in PEDOT:PSS can also improve its ability in guiding hole. They reported that the V_{oc} of the organic–inorganic hybrid silicon solar cell can be remarkably increased from 0.37 to 0.48 V after the PEDOT:PSS is doped with ZnP; meanwhile, the J_{sc} can be increased from 1.94 to 3.81 mA/cm^2. Consequently, the conversion efficiency can be increased by more than two times. Sorbitol is also a widely used dopant in PEDOT:PSS, which can enhance the conductivity of PEDOT:PSS thin films by three orders of magnitude [64].

Some organic compounds can also protect PEDOT:PSS from being polluted by water vapor; thus, it is helpful to improve the stability of the solar cells. For instance, A.M. Nardes et al. [64] found that, if we add sorbitol in PEDOT:PSS aqueous solution, the sorbitol can be dissolved out from the PEDOT:PSS material and form an individual film during the annealing process. Such sorbitol film can significantly reduce the tendency to take up water from the air, which increases the environmental stability and improves the efficiency of solar cell. The conductivity of such fabricated PEDOT:PSS film can almost be maintained constant for 2 h up to 45% relative humidity [64].

3.1.4 Preparation of Electrodes

The last step to fabricate the organic–inorganic hybrid silicon solar cells is to prepare the front and back electrodes. The function of the front electrode is to collect holes; meanwhile, ensure the area of the plate is facing the sun as much as possible (not shelter by the front electrode). In the organic–inorganic hybrid silicon solar cell, since the hole-transporting capacity of the PEDOT:PSS is not as good as expected, an ITO layer should be deposited on the PEDOT:PSS layer firstly to avoid the lateral transport of holes. Besides it can improve the hole collection efficiency, and the ITO layer can also act to protect the PEDOT:PSS from the water vapor. After that, the silver finger electrode (usually with 50 μm in width, 20 μm in height) will be screen printed on the ITO layer.

The function of the back electrode is to collect electrons. The most simple and common method is to plate an Ag or Al film with a thickness of about 100 nm on the back of the solar cell directly. However, it is hard to fabricate solar cells of high conversion efficiency using this method. This is because the thickness of the silicon substrate in this type of organic–inorganic hybrid silicon solar cells is too thin; thus, a large number of light-generated holes will diffuse to the region near the back electrode. Therefore, there will be a large carrier recombination on the interface between the silicon substrate and the back electrode.

An effective method to reduce the carrier recombination at this interface is to introduce a back electric field to prevent the hole from spreading to the back electrode. Through fabricating a back surface heavy doping layer (n^+) before depositing the silver rear electrode, He et al. [51] realized a 13.6% efficiency on 20-μm-thick organic–inorganic hybrid silicon solar cell. Zhang et al. [6] have made many efforts on building the back electric field using simple solution process under low temperature (~150 °C). They found that inserting a Liq (8-hydroxyquinolinolato-lithium) layer ~2 nm between the rear side of Si and the Al electrode can effectively enhance the Schottky barrier height and built-in voltage, thus reducing charge recombination. This Liq insert can improve the PCE of solar cells 29.5% (from 9.4% to 12.2%). A cesium carbonate (Cs_2CO_3) layer has also been tried to insert between Si and the rear electrode Al. The charge carrier recombination rates are effectively suppressed at the rear surface due to the deflection of holes, and a high PCE of 13.7% is achieved.

It should be noted that the edges of the device must be cut out after the electrodes have been fabricated to avoid short circuit.

3.2 Passivation Technologies on the Organic–Inorganic Interface

Passivation on the organic–inorganic interface is a very important step in fabricating organic–inorganic hybrid silicon solar cells. From transient and steady output characteristics measurement on the current density and voltage of the fabricated

silicon/PEDOT:PSS devices, Sun et al. [2] have confirmed that the surface passivation dominated the charge recombination process, thus playing a critical role on the device performance. Since it is inevitable to introduce abundant defects when we directly spin coat the organics on the silicon, the carrier recombination can be effectively reduced by passivation technique. Recent researches demonstrated that effective passivation on the organic–inorganic interface should be the bottleneck for achieving solar cells with high efficiency, and many passivation methods have been attempted.

Native oxidizing passivation method is the most commonly adopted method in the past organic–inorganic hybrid silicon solar cells. The cleaned silicon wafer only should be put under clean air condition for 12–24 h, and a uniform silica layer about 1.5 nm can be formed on the silicon surface. Such a silica layer can effectively passivate the surface defects, which results in that the minority lifetime on the silicon surface can reach about 26 μs [5]. Ye et al. [65] have developed the surface quality of the silica passivation layer using a simple and repeatable wet oxidation method. They found that the oxidizing aqueous solution of HNO_3 can introduce a uniform and dense silica thin layer on the silicon surface, which can provide better surface passivation and stronger wettability than that formed after native oxide. The HNO_3-oxidized device they fabricated displays better performance than in the native oxide case, with the PCE is enhanced by 28.96% (from 8.53% to 11%).

Besides, Sun et al. [2] have found that organic compounds can also be used as the passivation layer for the silicon/PEDOT:PSS interface. They have fabricated a methyl/allyl organic monolayer on the silicon nanowires by immersing chlorine terminated silicon nanowire substrate in an organic solution to graft the methyl/allyl. The charge carrier lifetime of the hybrid devices can be extended to 29.3 μs, and correspondingly the PCE of the device reaches 10.2%. Most recently, Li et al. [5] have found that the intrinsic amorphous silicon (i a-Si) passivation technique widely used in HIT solar cells can also perform well for the organic–inorganic hybrid silicon solar cells. An i a-Si layer of about 2 nm has been inserted (PECVD deposition) between the silicon surface and the PEDOT:PSS and obtained a minority lifetime about 45 μs. The short current density of the fabricated solar cell reached 83.0% of the theoretical limit. This is the best passivation effect that has been reported and thus should be a practical and effective passivation technique for high-efficiency organic–inorganic hybrid silicon solar cells.

Using atomic layer deposition (ALD) to deposit an Al_2O_3 thin film as the passivation layer is widely used to fabricate the organic–inorganic hybrid silicon solar cells with the radial heterojunction. This is because a conformal thin film can be achieved on high aspect ratio surface using the ALD method. Notably, the thickness of the Al_2O_3 layer should be thinner than 2.5 nm to avoid hindering the carrier transport. By depositing an Al_2O_3 passivation layer with thickness ~0.7 nm between the silicon nanocone array and the PEDOT:PSS layer, Pudasaini et al. [66] found that the interfacial defect density decreased 31.3%, and the PCE is enhanced from 9.65% to 10.56%.

3.3 Key Points in the Device Fabrication Process

As a summary, the fabrication of organic–inorganic hybrid silicon solar cells includes six key points.

1. The cleaning step is the basic process and the prerequisite for obtaining high-efficiency devices.
2. The modification of the silicon wafers and the PEDOT:PSS ensures the fabrication of good organic and inorganic heterojunction.
3. In the case that the above two steps have been perfectly completed, the preparation of the PEDOT:PSS film on the silicon substrate is one of the most important steps because the thickness of the film must balance the quality of heterojunction and electrical conductivity.
4. Storage of the silicon wafer with PEDOT:PSS layer isolated from water vapor is necessary since the PEDOT:PSS absorbs water which will seriously affect its performance.
5. The preparation of electrodes has great influence on the PCE of the devices obtained.
6. The passivation technique for the organic and inorganic interface should be paid special attentions on, which has been demonstrated to be the bottleneck limiting the PCE of the organic–inorganic hybrid silicon solar cells.

4 Conclusions

In this chapter, recent progress on the fabrication of ultrathin flexible crystal silicon membrane and several silicon nanostructures for light trapping and the detailed fabrication process including the key factors of organic–inorganic hybrid silicon solar cells are summarized. Preparation of crystalline silicon membrane is the premise as it is always adopted as the optical absorber in organic–inorganic hybrid silicon solar cells, while the silicon nanostructures are necessary to make up the insufficient light absorption in the ultrathin silicon. Till now, the fabrication processes of the ultrathin flexible crystal silicon membrane and the silicon nanostructures, using the wetting chemical etching methods, both have advanced to a level where desired thickness, size, and surface quality can be readily fabricated. The fabrication technique of the organic-inorganic hybrid silicon solar cells is very important to ensure the high efficiency. The fabrication steps are described in detail where six key points need to be paid attention are emphasized. For such organic–inorganic hybrid silicon solar cells, passivation techniques on the organic/silicon interface should be the bottleneck limiting the PCE. There are many efforts that have been made on this issue, but it still far away from being solved perfectly. We predict passivation must be the research highlight in the field of organic–inorganic hybrid silicon solar cells. Organic–inorganic hybrid silicon solar cells can reduce the cost, maintain high conversion efficiencies and good stability, and

obtain good mechanism flexibility; therefore, they should be a promising type of solar cells. We hope that the above contents can make a little bit of contribution to the photovoltaic field.

Acknowledgments This work is supported partially by National High-Tech R&D Program of China (863 Program, No. 2015AA034601), National Natural Science Foundation of China (Grant nos. 91333122, 51372082, 51402106, and 11504107), PhD Programs Foundation of Ministry of Education of China (Grant no. 20130036110012), Par-Eu Scholars Program, Beijing Municipal Commission of Science and Technology Project (Z161100002616039), and the Fundamental Research Funds for the Central Universities (2016JQ01, 2015ZZD03, 2015ZD07, 2017ZZD02).

References

1. P.C. Yu, C.Y. Tsai, J.K. Chang, C.C. Lai, P.H. Chen, Y.C. Lai, P.T. Tsai, M.C. Li, H.T. Pan, Y.Y. Huang, C.I. Wu, Y.L. Chueh, S.W. Chen, C.H. Du, S.F. Horng, H.F. Meng, ACS Nano **7**, 10780 (2013)
2. F. Zhang, D. Liu, Y. Zhang, H. Wei, T. Song, B. Sun, ACS Appl. Mater. Interfaces **5**, 4678 (2013)
3. M. Sharma, P.R. Pudasaini, F. Ruiz-Zepeda, D. Elam, A.A. Ayon, ACS Appl. Mater. Interfaces **6**, 4356 (2014)
4. J. He, P.Q. Gao, M.D. Liao, X. Yang, Z.Q. Ying, S.Q. Zhou, J.C. Ye, Y. Cui, ACS Nano **9**, 6522 (2015)
5. Y. Li, P. Fu, R. Li, M. Li, Y. Luo, D. Song, Appl. Surf. Sci. **366**, 494 (2016)
6. Y. Zhang, F. Zu, S.T. Lee, L. Liao, N. Zhao, B. Sun, Adv. Energy Mater. **4**, 2195 (2014)
7. W. Qiu, Dissertation, SiChuan Normal University, (2014)
8. F. Bai, M. Li, D. Song, H. Yu, B. Jiang, Y. Li, J. Solid State Chem. **196**, 596 (2012)
9. T. Huang, T. Yen, MRS Proceedings, 1302, mrsf10–1302-w1309–1304 , (2011)
10. C.Y. Chen, C.S. Wu, C.J. Chou, T.J. Yen, Adv. Mater. **20**, 3811 (2008)
11. L. Li, Y. Liu, X. Zhao, Z. Lin, C.-P. Wong, ACS Appl. Mater. Interfaces **6**, 575 (2013)
12. Z. Huang, T. Shimizu, S. Senz, Z. Zhang, N. Geyer, U. Gosele, J. Phys. Chem. C **114**, 10683 (2010)
13. F. Bai, M. Li, D. Song, H. Yu, B. Jiang, Y. Li, Appl. Surf. Sci. **273**, 107 (2013)
14. S. An, S.G. Lee, S.G. Park, E.H. Lee, O. Beom-Hoan, Sensor. Actuat. a-Phys. **209**, 124 (2014)
15. K.P. Rola, I. Zubel, J. Micromech. Microeng. **21**, 115026 (2011)
16. I. Zubel, M. Kramkowska, Sensor. Actuat. a-Phys. **101**, 255 (2002)
17. I. Zubel, K. Rola, M. Kramkowska, Sensor. Actuat. a-Phys. **171**, 436 (2011)
18. A. Splinter, J. Stürmann, W. Benecke, Mater. Sci. Eng. C **15**, 109 (2001)
19. K. Sato, M. Shikida, T. Yamashiro, M. Tsunekawa, S. Ito, Sensor. Actuat. a-Phys. **73**, 122 (1999)
20. B. Fan, F. Peng-Fei, C. Peng, H. Rui, L. Rui-Ke, Z. Zhi-Rong, Y. Hang, Z. Yan, S. Dan-Dan, L. Ying-Feng, J. Infrared Millim. W. **34**, 471 (2015)
21. K. Peng, Y. Xu, Y. Wu, Y. Yan, S.T. Lee, J. Zhu, Small **1**, 1062 (2005)
22. Y. Li, L. Yue, Y. Luo, W. Liu, M. Li, Opt. Express **24**, A1075 (2016)
23. Y. Li, M. Li, R. Li, P. Fu, T. Wang, Y. Luo, J.M. Mbengue, M. Trevor, Sci. Rep-Uk **6**, 24847 (2016)
24. I. Zardo, S. Conesa-Boj, S. Estradé, L. Yu, F. Peiro, P.R.i. Cabarrocas, J. Morante, J. Arbiol, A.F.i. Morral, Appl. Phys. A Mater **100**, 287 (2010)
25. S. Hofmann, C. Ducati, R. Neill, S. Piscanec, A. Ferrari, J. Geng, R. Dunin-Borkowski, J. Robertson, J. Appl. Phys. **94**, 6005 (2003)
26. D. Ma, C. Lee, F. Au, S. Tong, S. Lee, Science **299**, 1874 (2003)

27. J.R. Maiolo, B.M. Kayes, M.A. Filler, M.C. Putnam, M.D. Kelzenberg, H.A. Atwater, N.S. Lewis, J. Am. Chem. Soc. **129**, 12346 (2007)
28. Y. Wu, P. Yang, J. Am. Chem. Soc. **123**, 3165 (2001)
29. D. Kwak, H. Cho, W.-C. Yang, Phys. E. **37**, 153 (2007)
30. J. Bhardwaj, H. Ashraf, A. McQuarrie, Proc. Symp. Microstructures and microfabricated systems, ECS, 1–13 (1997)
31. R.M. Ng, T. Wang, F. Liu, X. Zuo, J. He, M. Chan, Elect. Device Lett. Ie **30**, 520 (2009)
32. K.-Q. Peng, Y.-J. Yan, S.-P. Gao, J. Zhu, Adv. Mater. **14**, 1164 (2002)
33. K.Q. Peng, Z.P. Huang, J. Zhu, Adv. Mater. **16**, 73 (2004)
34. K. Peng, J. Hu, Y. Yan, Y. Wu, H. Fang, Y. Xu, S. Lee, J. Zhu, Adv. Funct. Mater. **16**, 387 (2006)
35. H. Han, Z. Huang, W. Lee, Nano Today **9**, 271 (2014)
36. Z. Huang, N. Geyer, L. Liu, M. Li, P. Zhong, Nanotechnology **21**, 465301 (2010)
37. W. Chern, K. Hsu, I.S. Chun, B.P.D. Azeredo, N. Ahmed, K.-H. Kim, J.M. Zuo, N. Fang, P. Ferreira, X. Li, Nano Lett. **10**, 1582 (2010)
38. J. Tang, J. Shi, L. Zhou, Z. Ma, Nano-Micro. Lett. **3**, 129 (2011)
39. J. Huang, S.Y. Chiam, H.H. Tan, S. Wang, W.K. Chim, Chem. Mater. **22**, 4111 (2010)
40. X. Geng, M. Li, L. Zhao, P.W. Bohn, J. Electron. Mater. **40**, 2480 (2011)
41. Y.F. Li, M.C. Li, D.D. Song, H. Liu, B. Jiang, F. Bai, L.H. Chu, Nano Energy **11**, 756 (2015)
42. J. Yeom, D. Ratchford, C.R. Field, T.H. Brintlinger, P.E. Pehrsson, Adv. Funct. Mater. **24**, 106 (2014)
43. S. Su, L. Lin, Z. Li, J. Feng, Z. Zhang, Nanoscale Res. Lett. **8**(1), 405 (2013)
44. Z. Huang, H. Fang, J. Zhu, Adv. Mater. **19**, 744 (2007)
45. Y.F. Li, M.C. Li, R.K. Li, P.F. Fu, B. Jiang, D.D. Song, C. Shen, Y. Zhao, R. Huang, Opt. Commun. **355**, 6 (2015)
46. F. Leonard, A.A. Talin, Phys. Rev. Lett. **97**, 163 (2006)
47. F. Bai, Dissertation, Harbin institute of Technology, (2014)
48. H.D. Um, J.Y. Jung, H.S. Seo, K.T. Park, S.W. Jee, S.A. Moiz, J.H. Lee, Jpn. J. Appl. Phys. **49**, 04DN02 (2010)
49. Y.F. Li, M.C. Li, R.K. Li, P.F. Fu, L.H. Chu, D.D. Song, Appl. Phys. Lett. **106**, 091908 (2015)
50. E. Garnett, P.D. Yang, Nano Lett. **10**, 1082 (2010)
51. J. He, P. Gao, M. Liao, X. Yang, Z. Ying, S. Zhou, J. Ye, Y. Cui, ACS Nano **9**, 6522 (2015)
52. Y. Cho, M. Gwon, H.-H. Park, J. Kim, D.-W. Kim, Nanoscale **6**, 9568 (2014)
53. Y. Li, M. Li, P. Fu, R. Li, D. Song, C. Shen, Y. Zhao, Sci. Rep-Uk **5**, 11532 (2015)
54. H. Lin, H.-Y. Cheung, F. Xiu, F. Wang, S. Yip, N. Han, T. Hung, J. Zhou, J.C. Ho, C.-Y. Wong, J. Mater. Chem. A **1**, 9942 (2013)
55. F. Bai, M. Li, R. Huang, Y. Li, M. Trevor, K.P. Musselman, RSC Adv. **4**, 1794 (2014)
56. T. Ohmi, J. Electrochem. Soc. **143**, 2957 (1996)
57. H. Jin, C. Xingbi, Y. Chuanren, X. Wang, Semicond. Sci. Technol. **5**, 006 (1999)
58. Q. Liu, M. Ono, Z. Tang, R. Ishikawa, K. Ueno, H. Shirai, Appl. Phys. Lett. **100**, 183901 (2012)
59. Z. Wang, H. Yang, X. Xi, Q. Qiao, J. JI, G. Li, J. Funct. Mater. **38**, 393 (2007)
60. X. Shen, B. Sun, D. Liu, S.-T. Lee, J. Am. Chem. Soc. **133**, 19408 (2011)
61. Y. Kim, A.M. Ballantyne, J. Nelson, D.D. Bradley, Org. Electron. **10**, 205 (2009)
62. T.-R. Chou, S.-H. Chen, Y.-T. Chiang, Y.-T. Lin, C.-Y. Chao, J. Mater. Chem. C **3**, 3760 (2015)
63. Q.-L. Meng, F. Li, X. Xi, W. Qian, L. Que, J. JI, Y. Ding, G. Li, J. Artificial Crystal **39**, 670 (2010)
64. A.M. Nardes, M. Kemerink, M. De Kok, E. Vinken, K. Maturova, R. Janssen, Org. Electron. **9**, 727 (2008)
65. J. Sheng, K. Fan, D. Wang, C. Han, J. Fang, P. Gao, J. Ye, ACS Appl. Mater. Interfaces **6**, 16027 (2014)
66. P. Pudasaini, A. Ayon, J. Phys. Conf. Ser. **476**, 012140 (2013)